(NASA-CR-174434) RAIN VOLUME ESTIMATION OVER AREAS USING SATELLITE AND RADAR DATA Semiannual Report, 1 Jul. - 31 Dec. 1984 (South Dakota School of Mines and Technology) 25 p HC A02/MF A01 CSCL 04B G3/47

N85-19568

Unclas 14375

SEMI-ANNUAL REPORT ON GRANT NO. NAG 5-386

Rain Volume Estimation Over Areas Using Satellite and Radar Data

Period Covered: 1 July 1984 - 31 December 1984

Principal Investigators:

Andre A. Doneaud

South Dakota School of Mines and Technology

Rapid City, South Dakota 57701-3995

Thomas H. Vonder Haar

Colorado State University

Fort Collins, Colorado 80523

This is a summary of the work accomplished during the second half of 1984. Some results from work accomplished in January 1985 are included.

The main emphasis of the study is to investigate the feasibility of rain volume estimation using satellite data following a technique recently developed with radar data, called the Area Time Integral. To accomplish this task, case studies were selected (during January 1984 -- see 1st Semi-annual Report) on the basis of existing radar and satellite data sets which match in space and time. The radar and rapid scan GOES satellite data were collected during the Cooperative Convective Precipitation Experiment (CCOPE) and North Dakota Cloud Modification Project (NDCMP).

Four multicell clusters were analyzed in 1984. The small mesoscale areas of Austin and Houze (1972) or the mesoscale cloud systems described by Super and Heimbach (1980) as cells bigger than a cumulus cloud but smaller than a typical mesoscale convective complex were considered "clusters." Two clusters were selected on each day, 12 June and 2 July, as illustrated in Table 1. The 12 June clusters occurred during daytime, while the 2 July clusters during nighttime.

The radar data were on hand at the Institute of Atmospheric Sciences, South Dakota School of Mines and Technology. Magnetic tapes of digital satellite data were acquired by the Department of Atmospheric Sciences, Colorado State University, from the Bureau of Reclamation, the University of Wisconsin through the National Environmental Satellite Data Information Service (NESDIS), and the GOES data archive at CSU. The satellite data were processed at the IRIS/DRSES (Interactive Research Imaging System/Direct Readout Satellite Earth Station) facility located at CSU. The radar data were processed at SDSM&T. Details concerning data processing were

TABLE 1

No.	Cluster Identification	Date 1981	Time Period (GMT)	Satellite Data Type
1	1A	12 June	1627-1925	infrared, visible
2	1B	12 June	1716-1925	infrared, visible
3	X1	2 July	0035-0453	infrared
4	X2	2 July	0221-0434	infrared

described in the first semi-annual report. Once the satellite data were processed into IRIS, the routines for navigation remapping and smoothing of satellite images were performed. The visible counts were normalized for solar zenith angle. The GOES satellite infrared data are calibrated and give count values which can be related to equivalent black body temperatures. The radar data tapes were processed following procedures similar to those described by Schroeder and Klazura (1978). Digital printouts of the dBz-values at low-tilt angle were prepared and converted from radial to a rectangular coordinate system. A radar sector of interest was defined to delineate specific radar echo clusters for each radar time throughout the radar echo cluster lifetime. The radar sector of interest was used to locate the convective cluster responsible for the rainfall in the remapped satellite data. The radar echo clusters within the defined sectors of interest were identified by drawing a "box" around the cluster for each radar scan. The coordinate of the "boxes" were entered into a computer program that calculates the cluster echo areas of $\geq$ 25 dBz reflectivity thresholds and the corresponding radar ATI. The rain volume for each cluster was then computed using an optimized Z-R relationship (Smith et al., 1975). Next, a satellite sector of interest was defined by applying small adjustments to the radar sector using a manual processing technique. This was done to avoid cloud features suspected of not being detected by the radar. It was (and it will be) one of the most delicate and difficult tasks of this investigation because of the following considerations:

1) Satellite and radar systems respond to different characteristics of clouds at different atmospheric levels. During a cluster lifetime, the geometry of the cluster as viewed from a low-tilt radar scan and a satellite picture of the cloud top changes dramatically.

2) Time differences between satellite and radar data sets can vary by as much as 10 min during which the evolution of the convective system continues.

3) Spacial positioning of the satellite observations relative to the radar location necessitate error inclusion due to limited accuracy of geometric corrections.

4) Location correction for a cloud as a function of height above the earth's surface leads to further uncertainties.

5) Vertical wind shear advects the top of the clouds downwind from the location of the radar echo area. The direction of vertical wind shear is toward the northeast for the two case days.

6) Another consideration in definition of the matching satellite sector of interest involves the inclusion or exclusion of cirrus spissatus. If the cirrus

debris appeared to be completely detached horizontally from the radar echo cluster, the cirrus cloud cover was excluded from the satellite sector. A multicell cluster may experience regrowth during its lifetime. This was the case with cell 1A. On the other hand, if the radar echo cluster was closely associated with the cirrus spissatus, cirrus clouds were included in the satellite sector. Cell 1A, 12 June 1981, exhibited continual redevelopment on the southern flank.

The cirrus debris makes definition of the end of a cluster (as a convective entity) from the satellite images difficult. The best way to avoid such difficulty is to define the maximum development of the cluster and consider it as the ending time of the analysis. The ATI technique is also valid if only the growing period of the cluster's lifetime is considered (Doneaud et al., 1984). The time of the maximum development of the cluster should be determined using both satellite and radar data. With further research, it is hoped that only satellite data may be used for this purpose.

The satellite brightness and temperature pixel counts above defined thresholds within the satellite sector of interest were counted by computer and converted to area (one pixel = 2.47 km^2). Histograms of area versus brightness counts were produced for each satellite time step for each data type for the lifetime of the storm. Graphs are then constructed with the ordinate representing digital counts and the abscissa being area multipled by time intervals (km^2 x hrs). The abscissa represents the satellite ATI equivalent for the whole lifetime of the storm. A digital count area matching the radar area multiplied with the corresponding time interval is also determined. Such histograms were produced for the four analyzed clusters (Fig. 1-6).

Different radar and satellite quantities for every time step for the four clusters are listed in Tables 2-5. The step-by-step evolution of the echo area multiplied by the time interval and of the threshold count value reflect the multicell characteristics of the clusters, yet still exhibit similar trends, although there are time lags between radar and satellite data.

Trends of radar and satellite products (from Tables 2-5) are displayed in Figs. 7-14. The similarity of the evolution of these curves, as well as differences and lags between radar and satellite products, are evident.

Figures 7 and 8 display temporal evolution of satellite and radar characteristic quantities for cluster 1A. Two growing and two decaying periods are visible in the trends of the radar data emphasizing the multicell character of the cluster. A hint of the first growing period is present in the satellite data trend primarily because the clusters initial stage was overlaid by debris from previous activity. The temporal variation of the radar and satellite

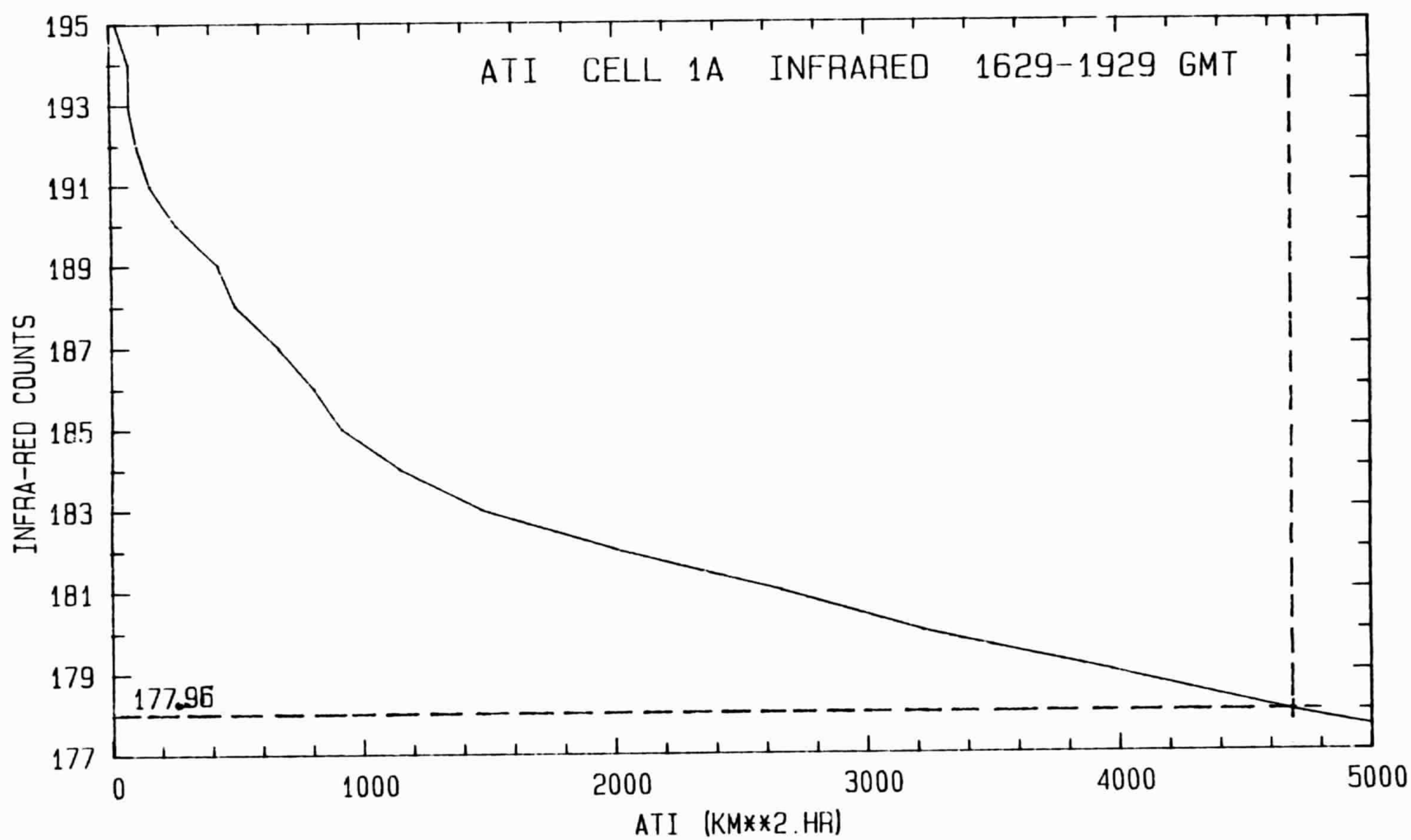

Fig. 1: Graph of ATI values for each satellite IR digital counts for cluster 1A. The dashed line represents the digital count for the satellite determined ATI.

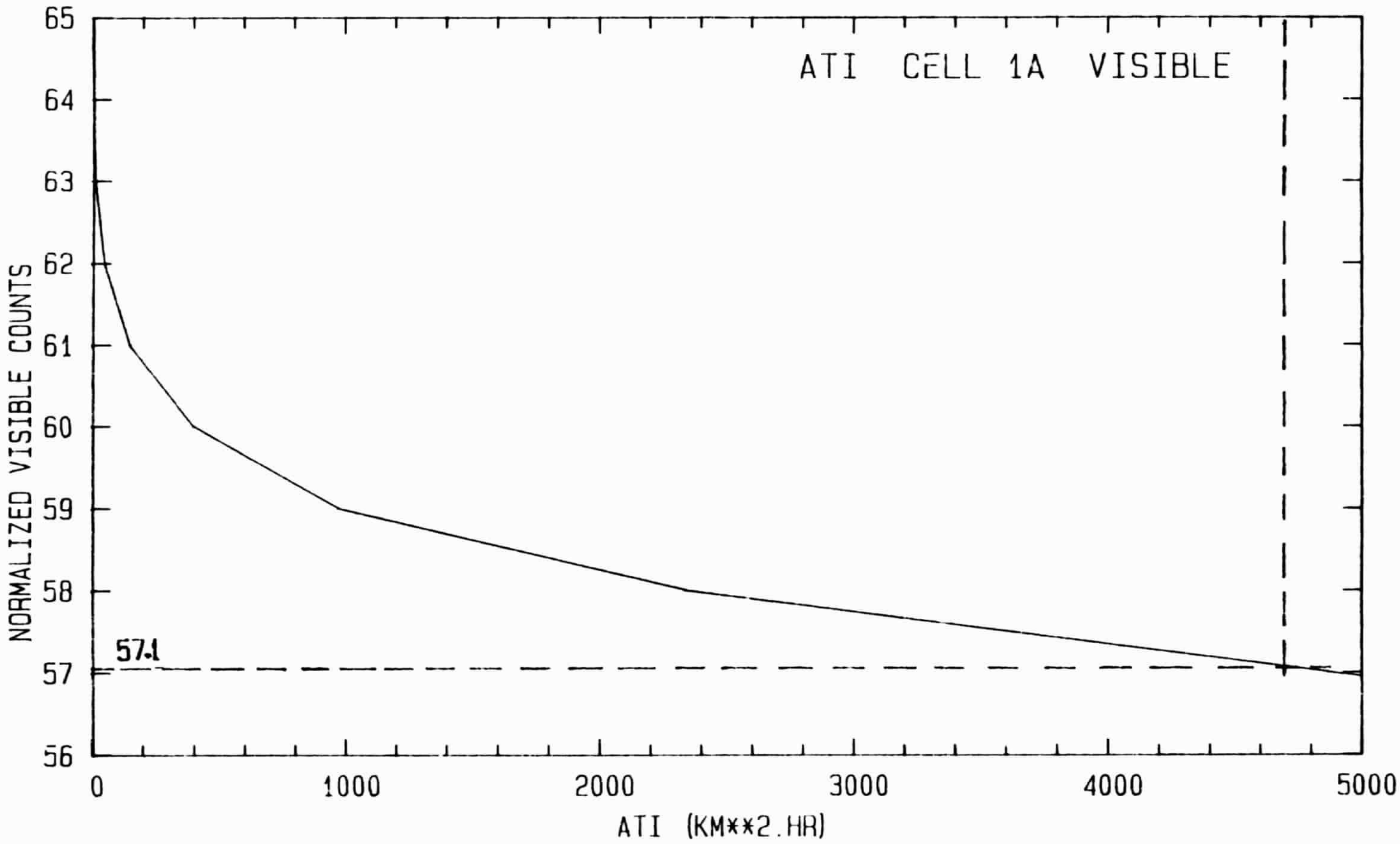

Fig. 2: Graph of ATI values for each satellite visible digital count for cluster 1A. The dashed line represents the digital count for the satellite determined ATI.

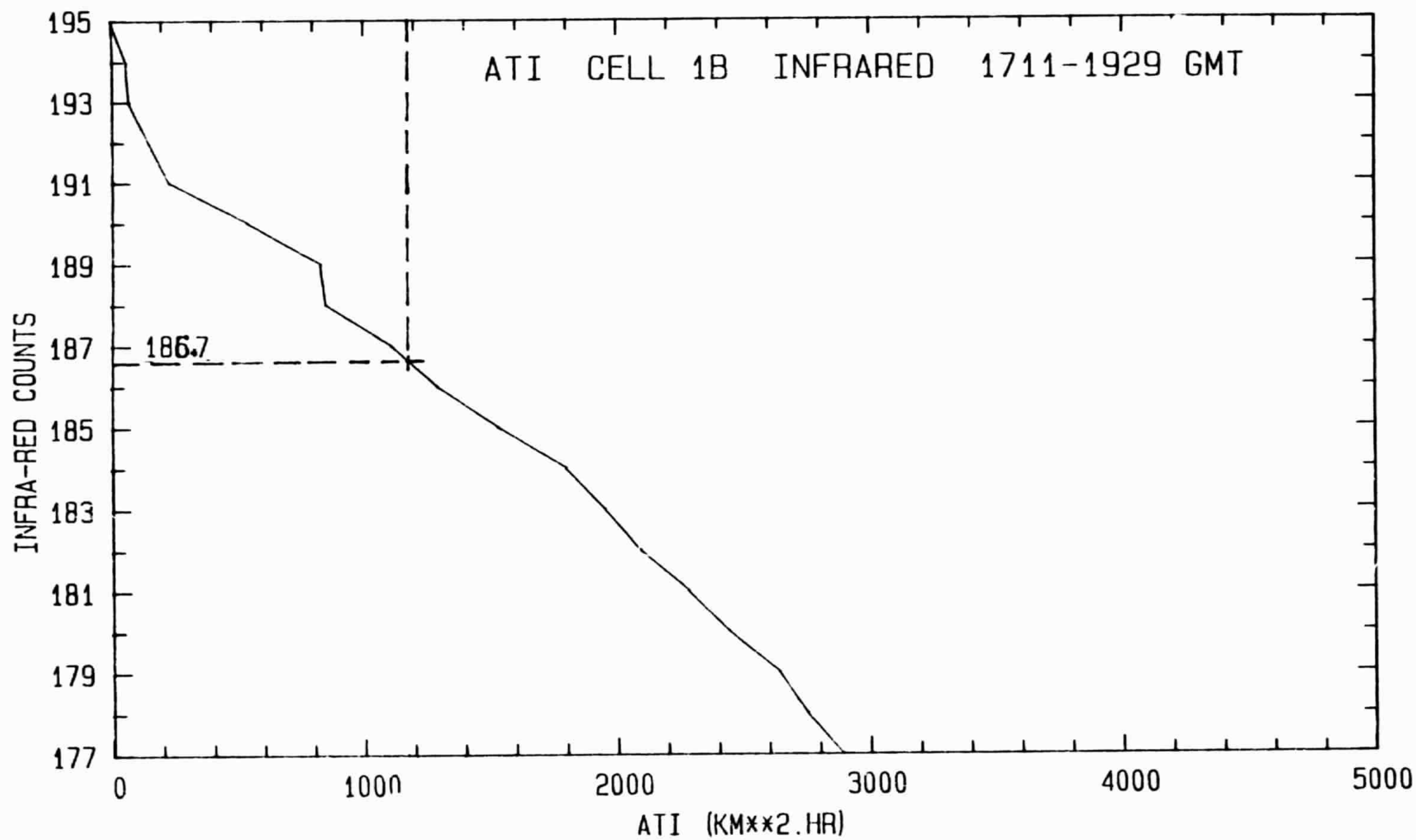

Fig. 3: Graph of ATI values for each satellite IR digital counts for cluster 1B. The dashed line represents the digital count for the satellite determined ATI.

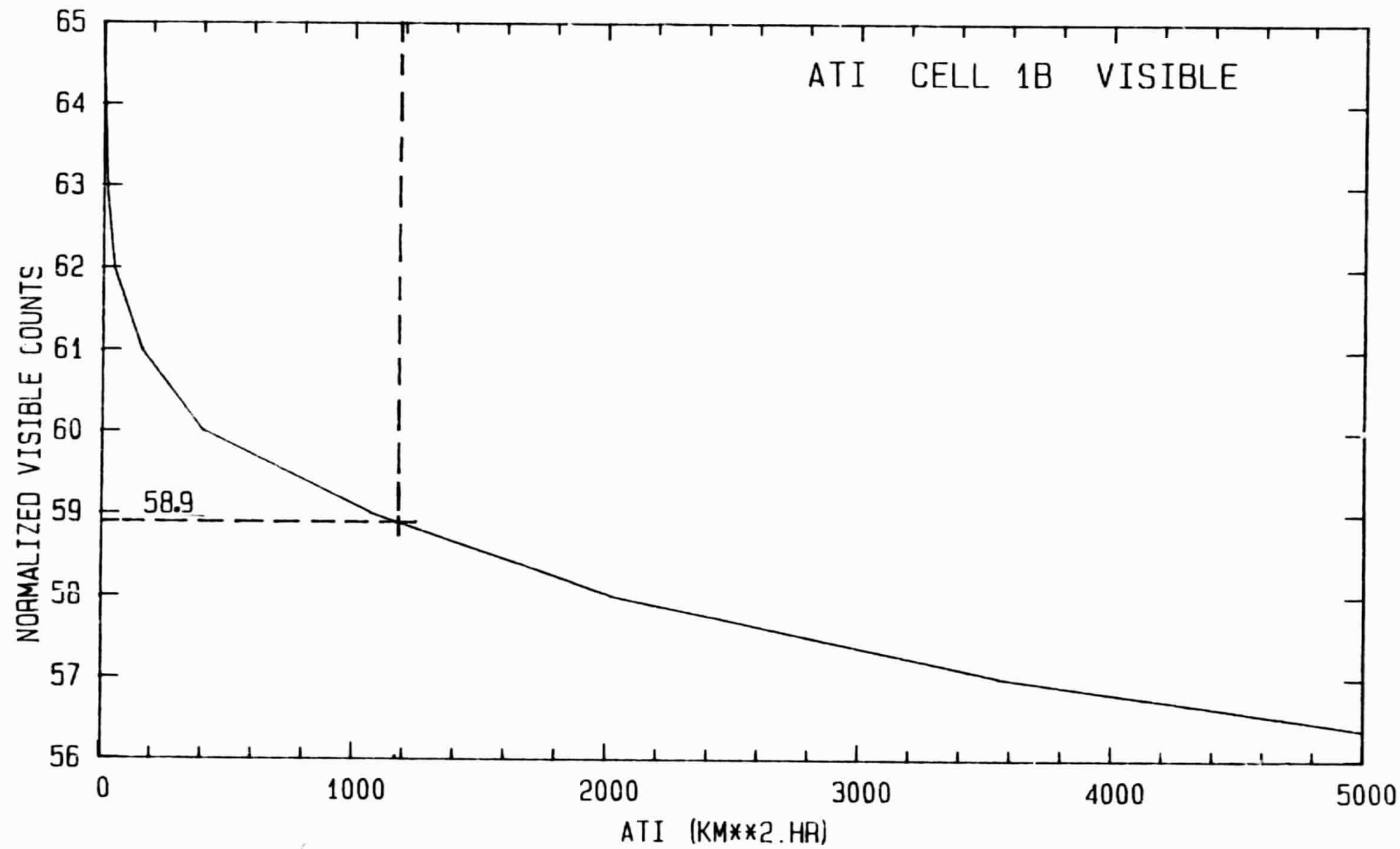

Fig. 4: Graph of ATI values for each satellite digital count for cluster 1B. The dashed line represents the digital count for the satellite determined ATI.

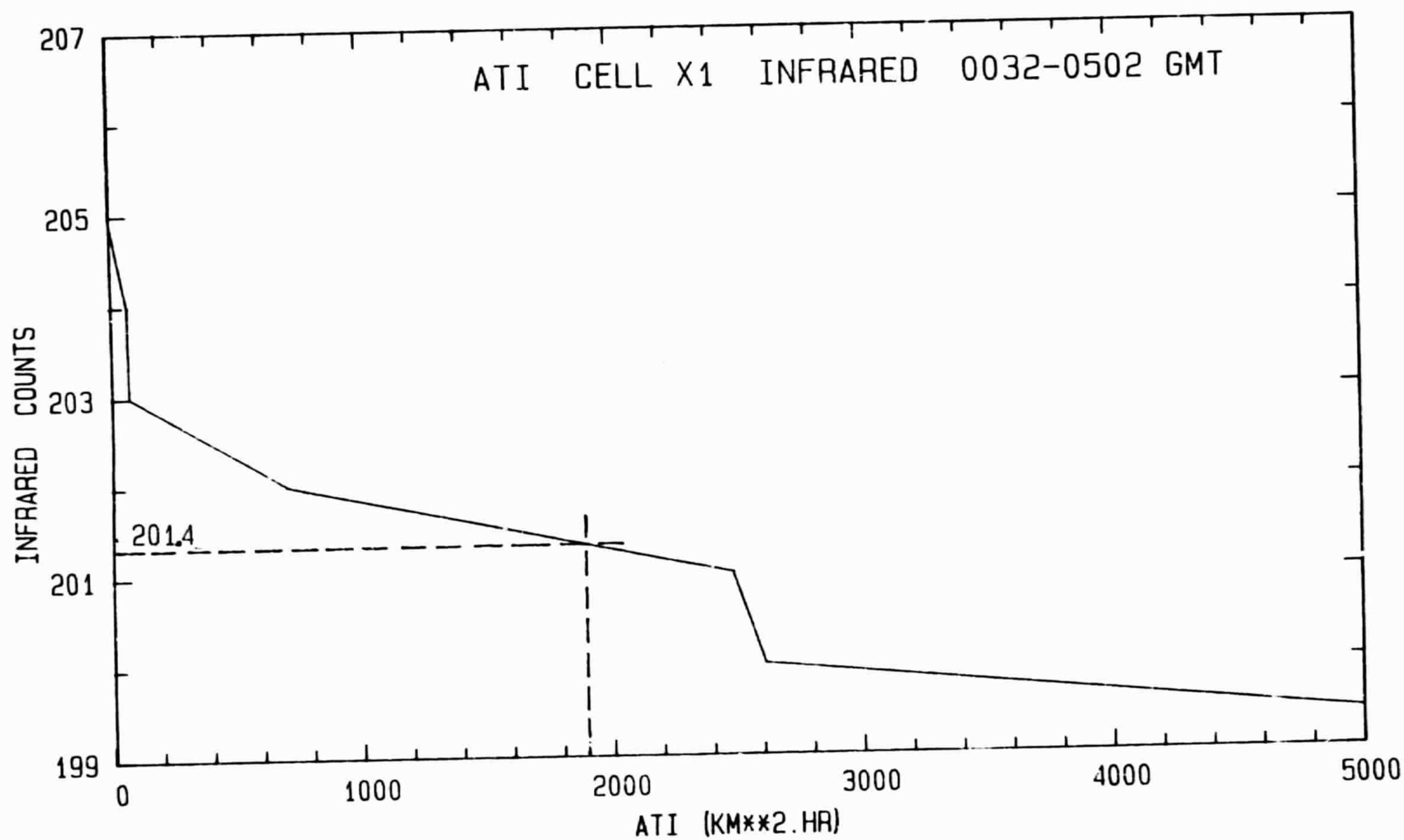

Fig. 5: Graph of ATI values for each satellite IR digital counts for cluster X1. The dashed line represents the digital count for the satellite determined ATI.

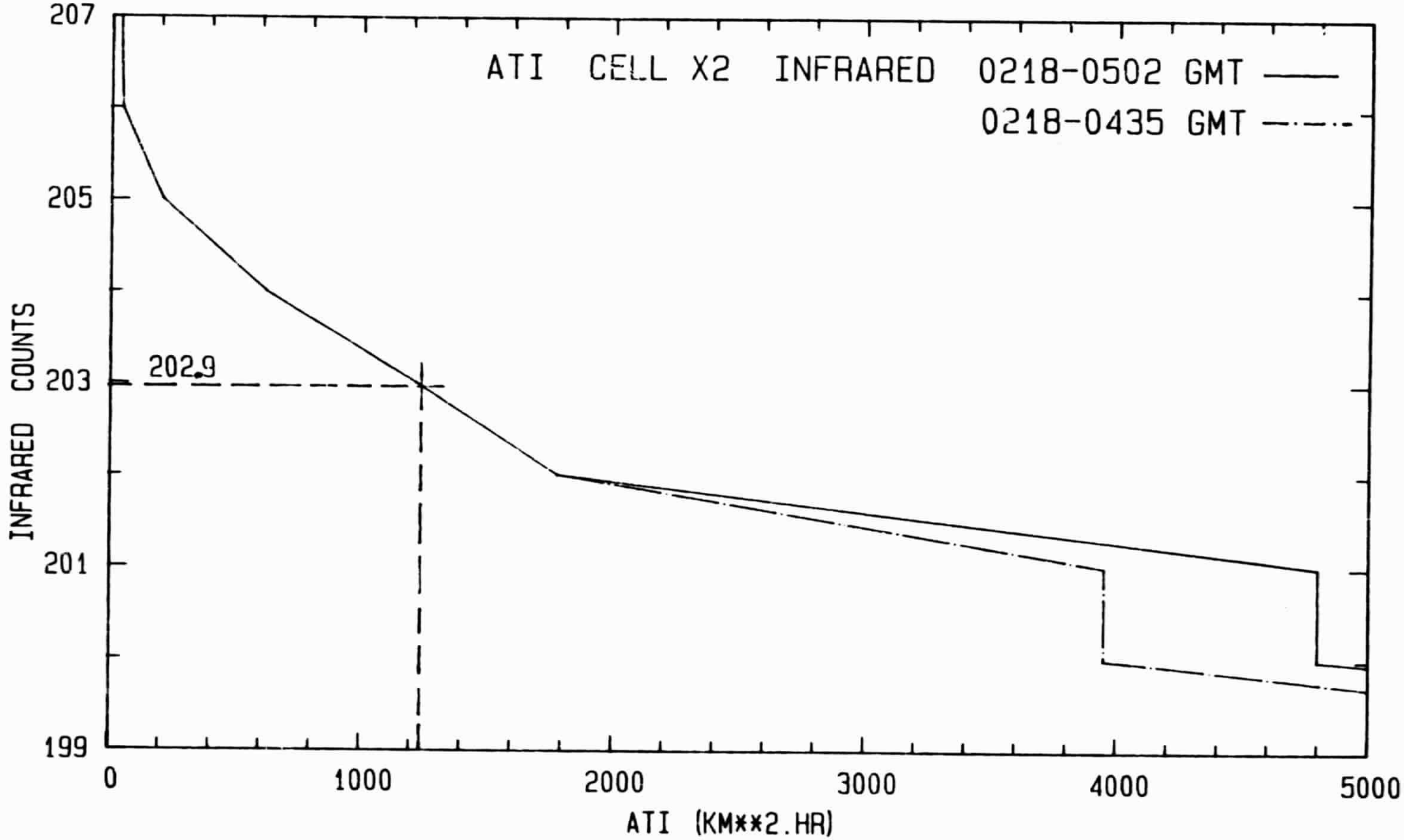

Fig. 6: Graph of ATI values for each satellite IR digital counts for cluster X2. The dashed line represents the digital count for the satellite determined ATI.

TABLE 2

CELL 1A. 12 June 1981

Bowman Radar Data

#	Time (GMT)	Δt (hr)	Area >25 dBz (km²)	Cum Area >25 dBz (km²)	Cum AT (km² hr)	Rain Vol. (mm km²)	Cum Rain Vol. (mm km²)	dBz MAX	MAX* Radar Ht (km)
1	1627	.09	1062	1062	96	692	692	47	8.3
2	1638	.18	1367	2429	342	799	1491	47	9.4
3	1649	.20	1569	3998	656	1013	2504	46	10.1
4	1702	.23	1820	5818	1075	1584	4088	56	9.3
5	1716	.25	2182	8000	1620	2176	6264	61	11.6
6	1732	.24	1789	9789	2050	1932	8196	61	12.0
7	1745	.20	1431	11220	2335	1244	9440	55	12.2
8	1756	.22	1097	12317	2578	858	10298	52	10.3
9	1811	.37	985	13302	2942	1063	11361	53	10.3
10	1828	--	--	--	--	--	--	--	--
11	1838	.29	2698	16000	3724	1690	13051	47	10.4
12	1848	.18	2002	18002	4085	1104	14155	48	8.6
13	1859	.22	2000	20002	4525	1502	15657	52	11.0
14	1915	.21	361	20363	4601	296	15953	43	8.7
15	1925	.08	300	20663	4625	166	16119	45	8.8

GOES Satellite Data

#	Time (GMT)	Satellite Time Increment Δts (hr)	Maximum Satellite Count Value: Visible	Maximum Satellite Count Value: Infrared	Maximum Satellite Count Value: Temp. (°C)	Interpolated Radar Area To Satellite Time (km²)	Interpolated Radar Area To Satellite Time: X Δts (km² hr)	Satellite Count Which Matches Interpolated Radar Area X Δts: Visible	Satellite Count Which Matches Interpolated Radar Area X Δts: Infrared	Satellite Count Which Matches Interpolated Radar Area X Δts: Temp. (°C)	Cumulative Satellite AT: AT (km² hr)
1	1629	.075	62	183	-38.2	1110	83.0	57.8	179.9	-35.1	83.0
2	1638	.100	61	183	-38.2	1367	136.4	56.9	178.9	-34.1	119.3
3	1641	.200	60	183	-38.2	1420	284.4	57.0	179.5	-34.7	503.8
4	1702	.250	60	183	-38.2	1820	455.0	56.6	179.9	-35.1	958.8
5	1711	.250	61	183	-38.2	2045	511.1	56.7	178.3	-33.5	1469.8
6	1732	.225	63	182	-37.2	1789	402.6	56.7	179.2	-34.4	1872.4
7	1738	.225	64	184	-39.2	1630	366.9	56.8	179.1	-34.3	2239.3
8	1759	.250	62	186	-41.2	1075	268.6	56.3	163.8	-25.1	2508.0
9	1808	.250	[illegible]	189	-44.2	1005	251.3	56.5	163.7	-25.1	2759.2
10	1829	.250	63	195	-50.2	2120	530.0	55.9	160.5	-23.5	3289.2
11	1838	.100	63	195	-50.2	2698	269.1	56.6	158.4	-22.4	3558.3
12	1841	.203	63	194	-49.2	2480	503.8	57.0	163.5	-25.0	4062.1
13	1902	.306	61	190	-45.2	1710	523.3	58.2	177.5	-32.7	4585.4
14	1918	.222	62	167	-26.7	345	77.8	59.5	151.2	-18.8	4663.2
15	1929	.094	64	158	-22.2	280	26.5	60.7	154.0	-20.2	4689.7

· Total duration of the cell is: 2.96 hrs.

· ATI is: 4,625 km² hr (radar); 4689.7 km² hr (satellite).

· Total Rain Volume is: 16,119 km² mm.

* dBz≥20

TABLE 3

CELL 1B 12 June 1981

	Bowman Radar Data									GOES Satellite Data											
											Satellite Time Increment	Maximum Satellite Count Value			Interpolated Radar Area To Satellite Time		Satellite Count Which Matches Interpolated Radar Area X Δts			Cumulative Satellite AT
#	Time (GMT)	Δt (hr)	Area >25 dBz (km²)	Cum Area >25 dBz (km²)	Cum AT (km² hr)	Rain Vol. (mm km²)	Cum Rain Vol. (mm km²)	dBz MAX	MAX* Radar Ht (km)	Time (GMT)	Δts (hr)	Visible	Infrared	Temp. (°C)	(km²)	X Δts (km²hr)	Visible	Infrared	Temp. (°C)	AT (km²hr)
1	1716	.08	350	350	28	327	327	47	8.9	1711	.175	57	146	-16.2	250	43.8	55.1	143.4	-14.9	43.8
2	1732	.23	557	907	156	672	999	57	11.0	1732	.225	59	154	-20.2	557	125.3	55.1	146.2	-16.3	169.1
3	1745	.20	649	1556	286	603	1602	49	12.1	1738	.225	60	156	-21.2	602	135.5	56.4	146.9	-16.6	304.6
4	1756	.22	529	2085	402	359	1961	48	9.9	1759	.250	64	176	-31.2	555	138.7	57.2	151.9	[illegible]	443.3
5	181[illegible]	.35	660	2745	633	770	2731	45	9.2	1808	.250	65	183	-38.2	632	158.0	57.8	170.3	-28.4	601.3
6	1828	--	--	--	--	--	--	--	--	1829	.250	64	194	-49.2	785	196.3	58.8	183.3	-38.5	797.6
7	1838	.32	860	3605	908	807	3538	38	8.5	1838	.100	63	192	-47.2	860	85.8	58.6	185.6	-40.8	883.4
8	1848	.17	515	4120	996	226	3764	37	7.8	1841	.203	63	194	-49.2	765	155.4	59.0	189.3	-44.5	[illegible].8
9	1859	.23	391	4511	1086	225	3989	40	8.4	1902	.306	63	190	-45.2	342	104.7	59.9	190.0	-45.2	1143.5
10	1915	.22	122	4633	1113	68	4057	34	6.8	1918	.222	61	194	-49.2	106	23.6	60.5	192.7	-47.9	1167.1
11	1925	.08	60	4693	1117	25	4082	32	6.5	1929	.094	62	191	-46.2	35	3.3	62.5	191.2	-46.2	1170.4

- Total duration of the cell is 2.5 hrs (2 hrs 29 min).
- ATI is: 1117 km² hr (radar); 1170.4 km² hr (satellite).
- Total RFR is: 4032 km² mm.

* dBz≥20

TABLE 4

CELL 11 2 July 1981

	Bowman Radar Data										GOES Satellite Data									
												Satellite Time Increment	Maximum Satellite Count V.		Interpolated Radar Area To Satellite Time		Satellite Count Which Matches Interpolated Radar Area X Δts		Cumulative Satellite AT
#	Time (GMT)	Δt (hr)	Area >25 dBz (km^2)	Cum Area >25 dBz (km^2)	Cum AT (km^2 hr)	Rain Vol. (mm km^2)	Cum Rain Vol. (mm km^2)	Z_e MAX	MAX* Radar Ht (km)	Time (GMT)	Δts (hr)	Infrared	Temp. (°C)	(km^2)	X Δts (km^2hr)	Infrared	Temp. (°C)	AT (km^2hr)
1	0035	.107	8	8	1	10	10	37	7	0032	.075	202	-57.2	0	0	203.0	-58.2	0
2	0047	.237	64	72	16	90	100	41	11.6	0041	.253	202	-57.2	41	10.4	202.9	-58.1	10.4
3	0103	.254	261	333	82	426	526	47	10.8	0103	.305	202	-57.2	262	80.0	200.6	-55.8	90.4
4	0118	.227	616	949	222	793	1319	47	11.7	0118	.222	204	-59.2	616	137.5	201.9	-57.1	227.9
5	0130	.245	686	1635	390	991	2310	53	10.8	0129	.250	204	-59.2	686	171.5	202.0	-57.2	399.4
6	0147	.260	596	2231	545	819	3129	54	12.5	0148	.405	202	-57.2	650	263.3	201.7	-56.9	662.7
7	0201	.280	1018	3249	830	1529	4658	51	9.8	M								
8	0221	.250	935	4184	1064	1508	6166	57	10.8	0218	.344	202	-57.2	946	325.4	201.1	-56.3	988.1
9	0231	.183	839	5023	1217	778	5944	50	11.1	0229	.194	204	-59.2	850	165.0	201.4	-56.6	1153.1
10	0243	.189	650	5673	1340	604	7548	50	11.2	0241	.250	201	-56.2	665	166.3	201.3	-56.5	1319.4
11	0254	.213	651	6324	1478	633	8181	49	10.7	0259	.225	198	-53.2	590	132.8	199.1	-54.3	1452.2
12	0308	.268	508	6832	1614	603	8784	46	8.9	0308	.300	198	-53.2	503	150.9	198.4	-53.6	1603.1
13	0326	.229	323	7155	1688	338	9122	45	9.9	M								
14	0336	.175	185	7340	1721	168	9290	44	9.5	0325	.331	196	-51.2	185	61.2	196.6	-51.8	1664.3
15	0347	.190	130	7470	1746	104	9334	38	10.4	0348	.355	195	-50.2	130	46.2	193.7	-50.9	1710.5
16	0358	.204	131	7601	1772	161	9555	42	7.7	M								
17	0412	.204	90	7691	1791	112	9667	44	9.7	0418	.344	195	-50.2	117	40.3	195.0	-50.2	1750.8
18	0423	.185	142	7833	1817	215	9882	48	10.6	0429	.144	194	-49.2	147	21.2	194.0	-49.2	1772.0
19	0434	.184	152	7985	1845	224	10106	45	6.9	0435	.155	192	-47.2	174	27.0	191.7	-46.3	1799.0
20	0445	.1[illegible]8	288	8273	1890	370	10476	48	9.5	0448	.129	195	-50.2	276	63.2	192.3	-47.5	1862.2
21	0453	064	263	8536	1907	275	10751	48	10.1	0503	.123	190	-45.2	226	27.8	189.4	-44.6	1890.0

Total Cell Duration: 4.30 hrs.

ATI: 1,907 km^2 hr (radar); 1,890 km^2 hr (satellite).

Total Rain Volume: 10,751 km^2 mm.

TABLE 5

CELL X2 2 July 1981

	Bowman Radar Data									GOES Satellite Data										
											Satellite Time Increment	Maximum Satellite Count Value		Interpolated Radar Area To Satellite Time		Satellite Count Which Matches Interpolated Radar Area X Δts		Cumulative Satellite AT
#	Time (GMT)	Δt (hr)	Area >25 dBz (km^2)	Cum Area >25 dBz (km^2)	Cum AT (km^2 hr)	Rain Vol. (mm km^2)	Cum Rain Vol. (mm km^2)	Z_e MAX	MAX* Radar Ht (km)	Time (GMT)	Δts (hr)	Infrared	Temp. (°C)	(km^2)	X Δts (km^2hr)	Infrared	Temp. (°C)	AT (km^2hr)
1	0221	.125	459	459	57	688	688	52	11.5	0218	.094	204	-59.2	437	41.1	199.8	-55.0	41.1
2	0231	.183	508	967	150	712	1400	53	9.7	0229	.194	202	-57.2	504	97.8	199.4	-54.6	138.9
3	0243	.189	725	1692	287	915	2315	53	12.2	0241	.250	202	-57.2	705	176.3	200.0	-55.2	315.2
4	0254	.213	976	2668	495	1660	3975	55	14.4	0258	.225	205	-60.2	890	200.3	201.2	-56.4	515.5
5	0308	.268	769	3437	701	1636	5611	54	12.8	0308	.300	207	-61.2	769	230.7	201.9	-57.1	746.2
6	0326	.229	792	4229	882	1010	6621	54	12.6	M								
7	0336	.175	769	4998	1017	814	7435	51	10.9	0335	.331	205	-60.2	769	254.5	204.2	-59.4	1000.7
8	0347	.190	610	5608	1133	630	8065	46	10.8	0348	.355	204	-59.2	565	200.6	202.8	-58.0	1201.3
9	0358	.204	246	5854	1183	298	8363	44	8.5	M								
10	0412	.204	211	6065	1227	278	8641	41	11.0	0418	.344	202	-57.2	117	40.2	202.8	-58.0	1241.5
11	0423	.185	49	6114	1236	58	8699	41	9.0	0429	.144	202	-57.2	20	2.9	202.9	-58.1	1244.4
12	0434	.092	2	6116	1236	2	8701	36	8.4	0435	.050	202	-57.2	0	0	203.0	-58.2	1244.4

Total Cell Duration: 2.22 hrs.

ATI: 1,236 km^2hr (radar); 1,244.4 km^2 hr (satellite).

Total Rain Volume: 8,701 km^2 mm.

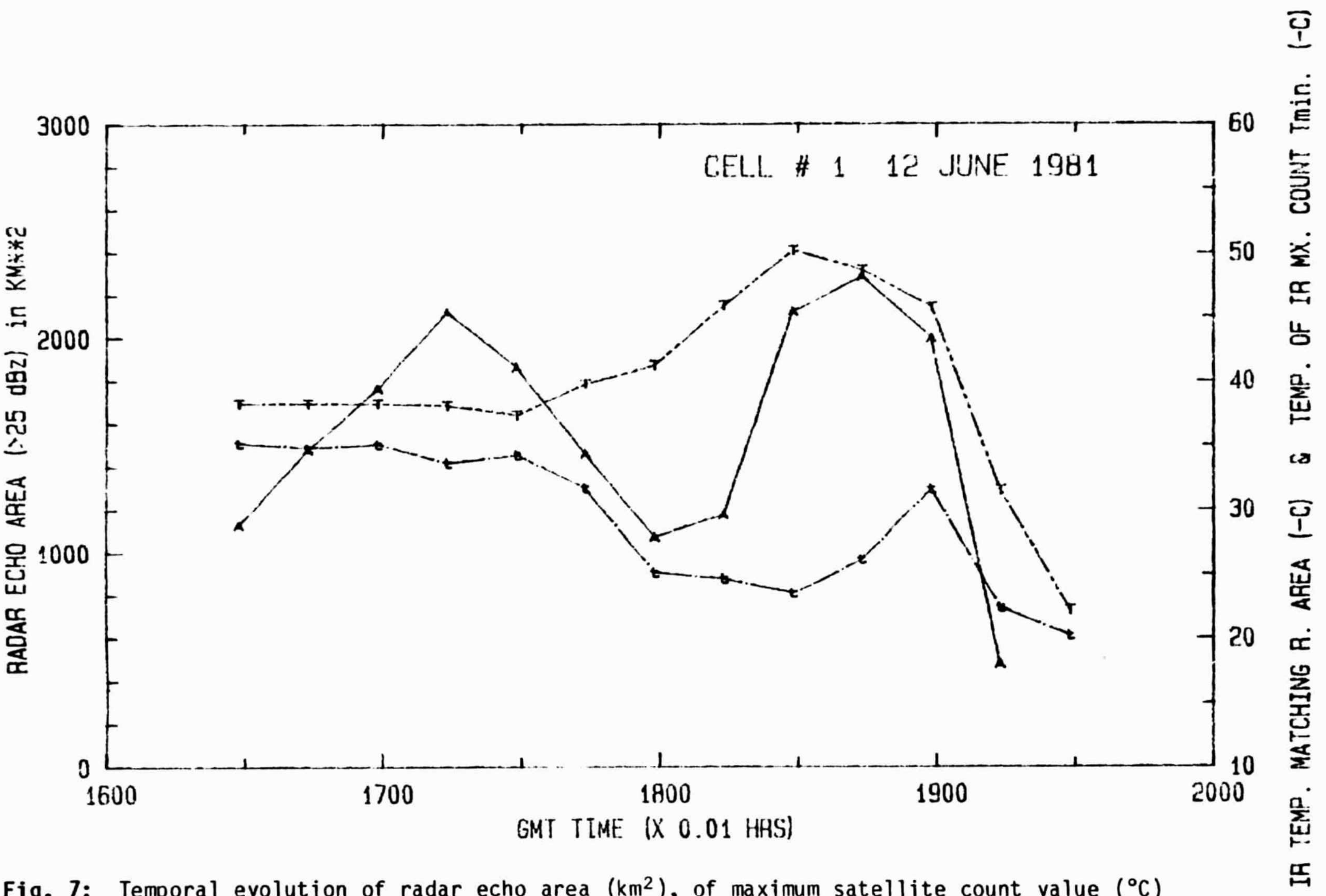

Fig. 7: Temporal evolution of radar echo area (km^2), of maximum satellite count value (°C) and of satellite count value (°C), matching the interpolated radar area multipled with time increment for cluster 1A.

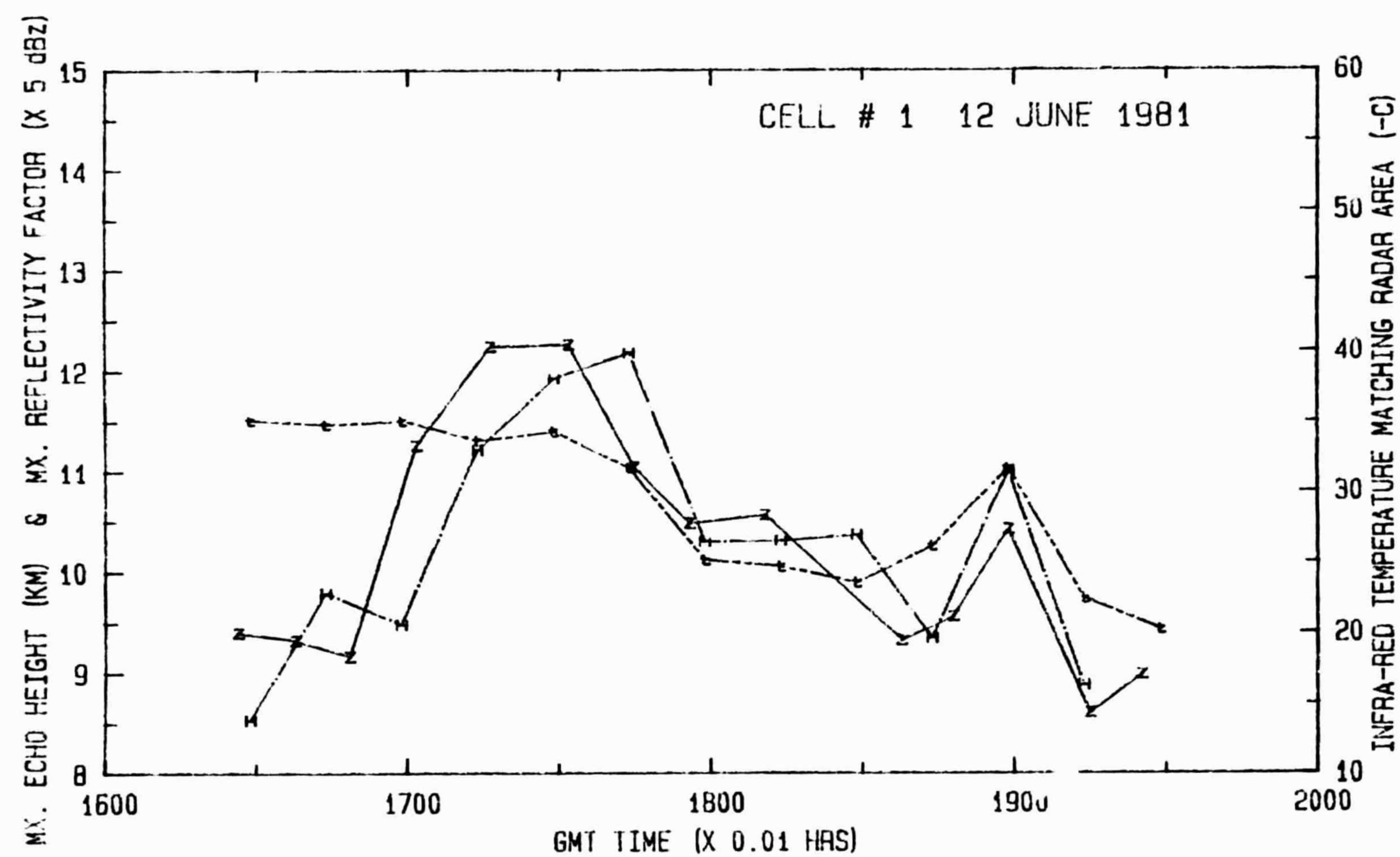

Fig. 8: Temporal evolution of maximum echo height, of maximum reflectivity factor (dBz) and of satellite count value (°C), matching the interpolated radar area multiplied with time increment for cluster 1A.

characteristic variables for cluster 1B is presented in Figs. 9 and 10. The radar echo area, the IR maximum counts, and the IR counts matching radar echo areas evolve similarly (Fig. 9), except for the decaying phase of the cluster where the cirrus debris keeps the IR counts high. The maximum echo height and the maximum reflectivity trends (Fig. 10) are opposite to the IR count matching radar area. Radar trends imply that a weak secondary peak is co-located with the peak in the IR count trend. Again these differences have to be attributed to the multicell nature of cluster 1B. The temporal evolution of the radar and satellite data for cluster X1 are displayed in Figs. 11 and 12. The trends are similar except for the initial stage of the cluster. Remnants of previous activity preclude initial observations. The cluster X2 (Figs. 13 and 14) demonstrates a growing and a decaying period. Its multicell character is self evident as the growth and decay of individual cells are indicated. Time lags of maximum development between radar and satellite variables is also evident.

The principal goal of this investigation is to compute convective rain volumes over stationary or floating target areas by considering independent satellite data. As such, the key element is to determine ATI from satellite data without using radar returns (as was done here). A satellite quantity defining the most appropriate digital count matching the radar ATI for a given cluster needs to be found. For instance, curves correlating satellite digital count thresholds (matching radar ATI's) and satellite IR maximum count values (°C) or satellite IR maximum count values (°C) averaged over the duration of the cell (or only its growing period) have to be identified. Such quantities for the four clusters analyzed are listed in Table 6. It is evident that the digital counts matching the radar ATI's are a function of cluster characteristics. Similarities between evolution of satellite counts matching radar ATI values and satellite IR maximum count values do exist; though cell 1A (which was not entirely recorded in the radar screen) seems to be an outlier. Certainly only four clusters are far from being sufficient for a correlative analysis. Work is continuing. Some other 5-6 clusters are scheduled to be processed and analyzed in 1985.

* * * * * * * * * * *

An extended abstract of the project's progress has been published in "Global Scale Atmospheric Processes Research Program Review" held at the NASA Goddard Space Flight Center, Greenbelt, Maryland, August 8-10, 1984, pp. 203-209.

A manuscript entitled "Convective Rain Rates and Their Evolution During Storms in a Semi-Arid Climate" coauthored by A. A. Doneaud, S. Ionescu-Niscov, and J. R. Miller, Jr., has been published in the August issue of the Mon. Wea. Rev., 112, 8, 1602-1612.

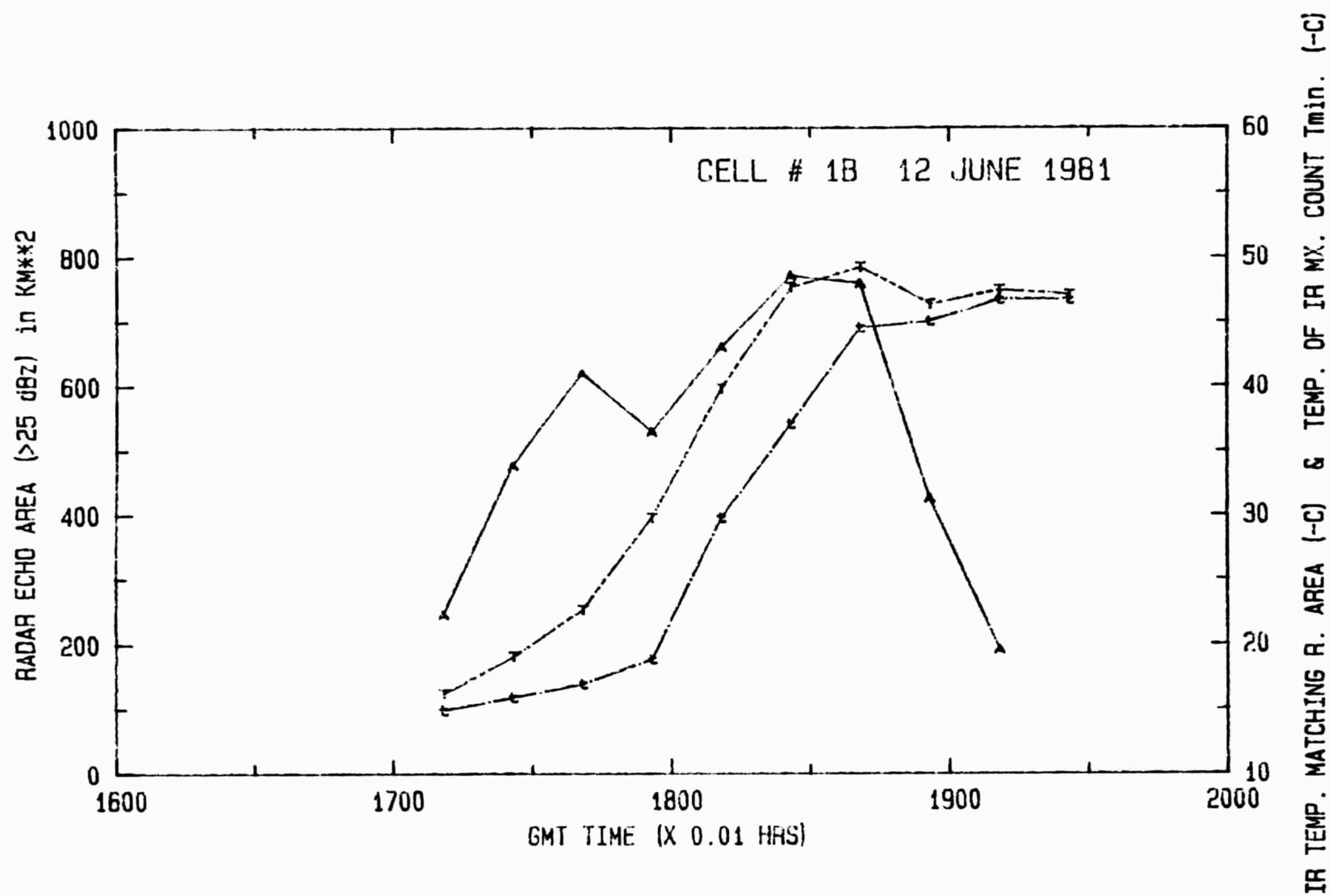

Fig. 9: Temporal evolution of radar echo area (km^2) of maximum satellite count value (°C) and of satellite count value (°C), matching the interpolated radar area multipled with time increment for cluster 1B.

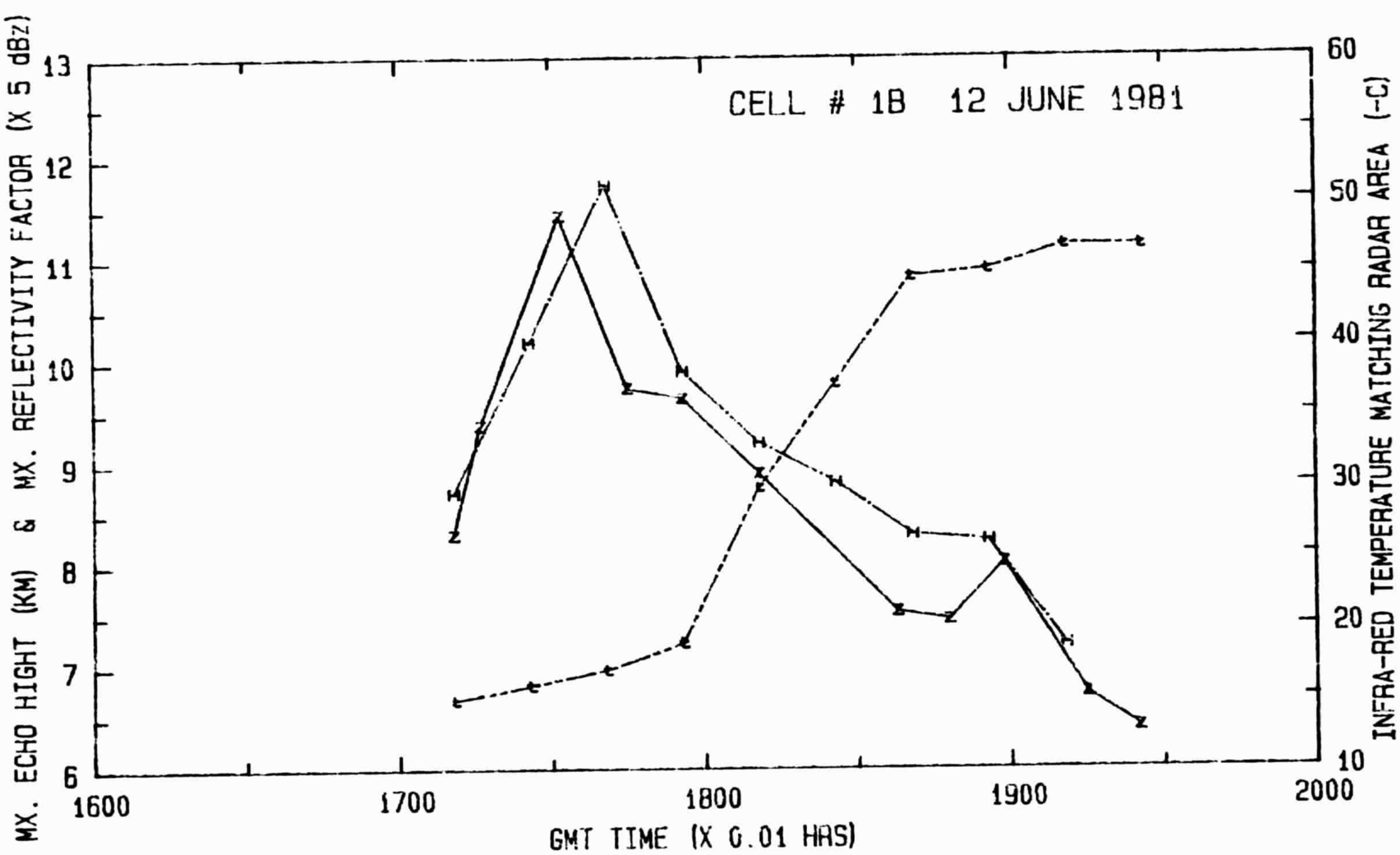

Fig. 10: Temporal evolution of maximum echo height, of maximum reflectivity factor (dBz) and of satellite count value (°C), matching the interpolated radar area multiplied with time increment for cluster 1B.

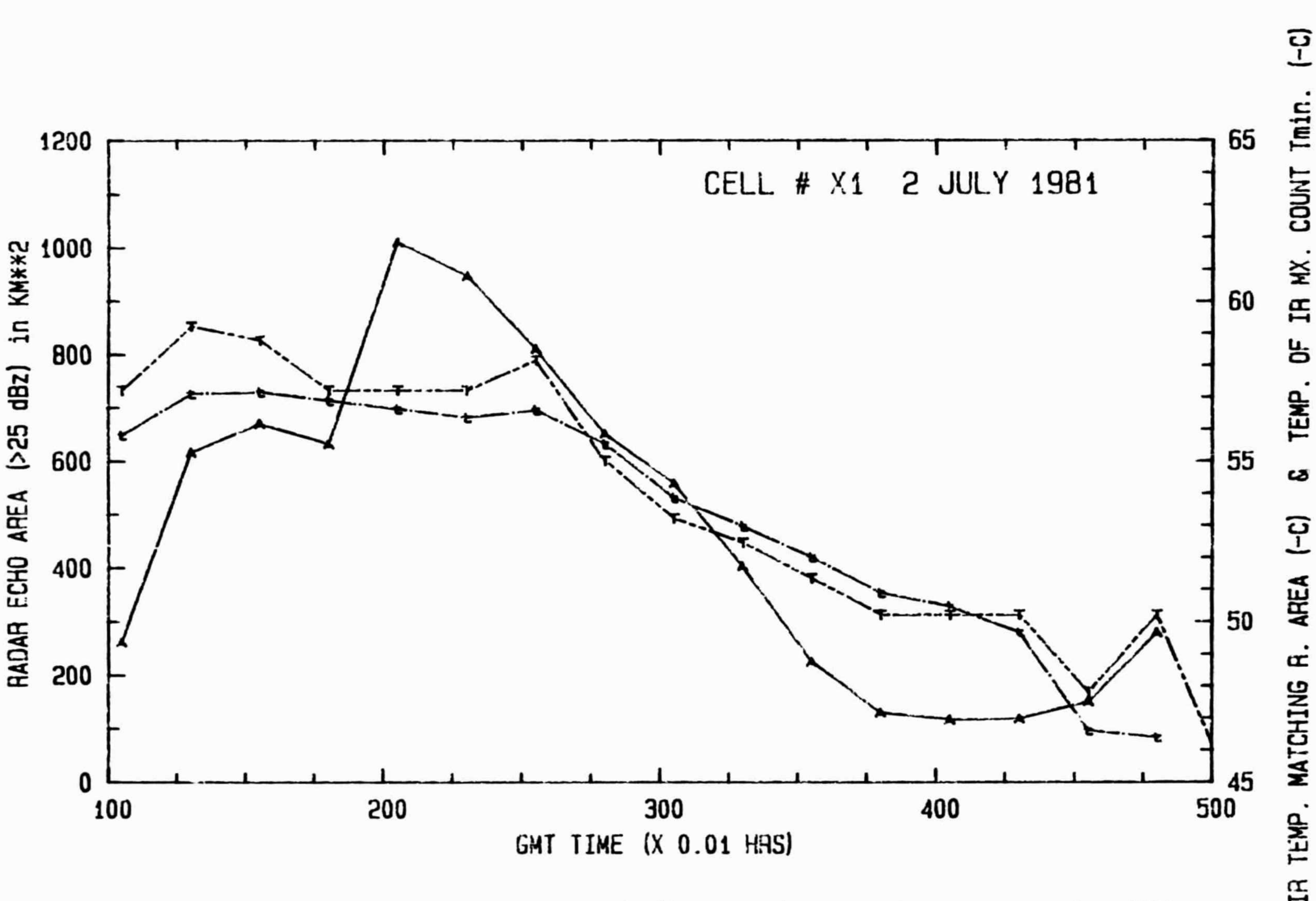

Fig. 11: Temporal evolution of radar echo area (km^2), of maximum satellite count value (°C) and of satellite count value (°C), matching the interpolated radar area multipled with time increment for cluster X1.

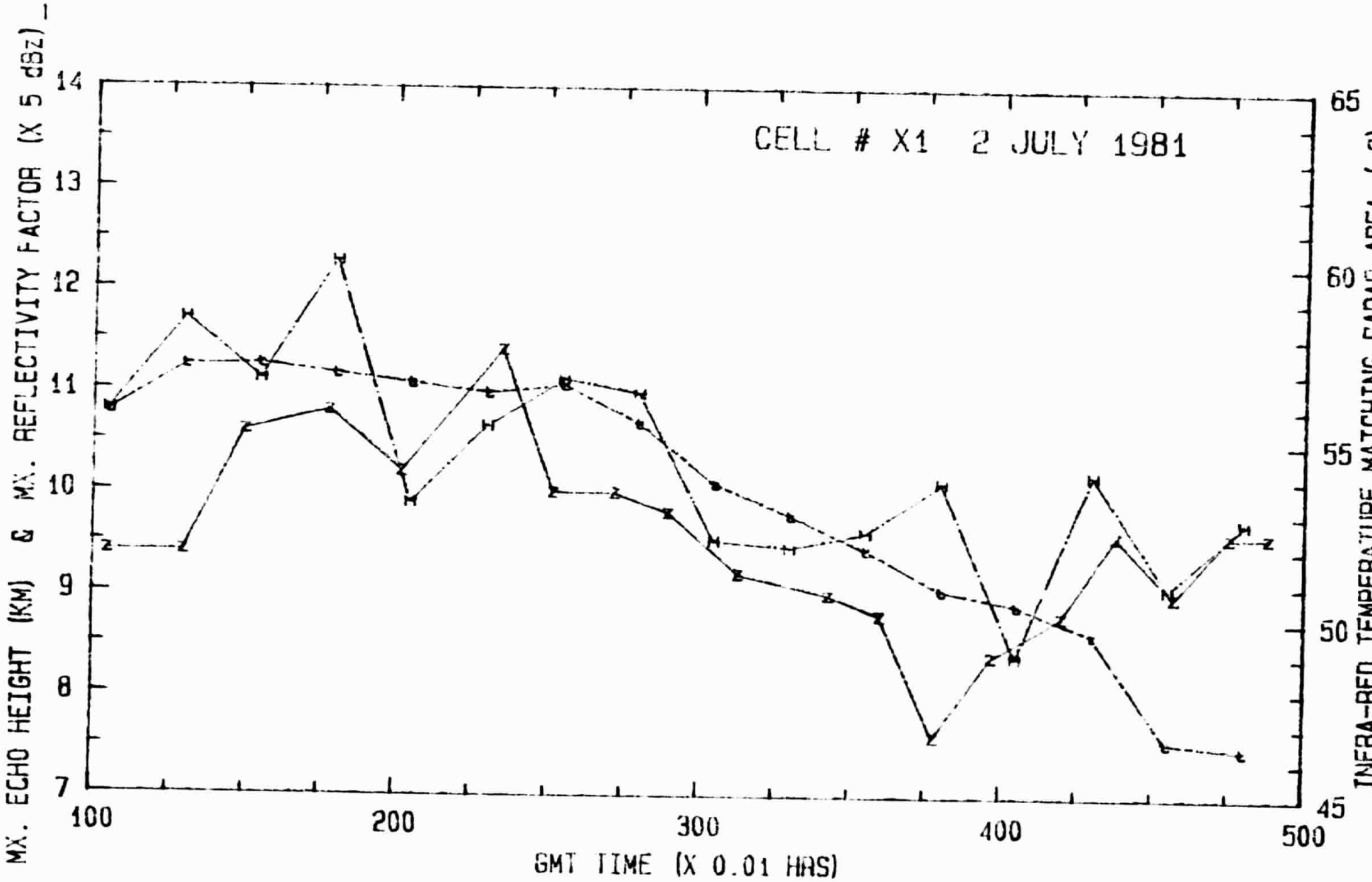

Fig. 12: Temporal evolution of maximum echo height, of maximum reflectivity factor (dBz) and of satellite count value (°C), matching the interpolated radar area multiplied with time increment for cluster X1.

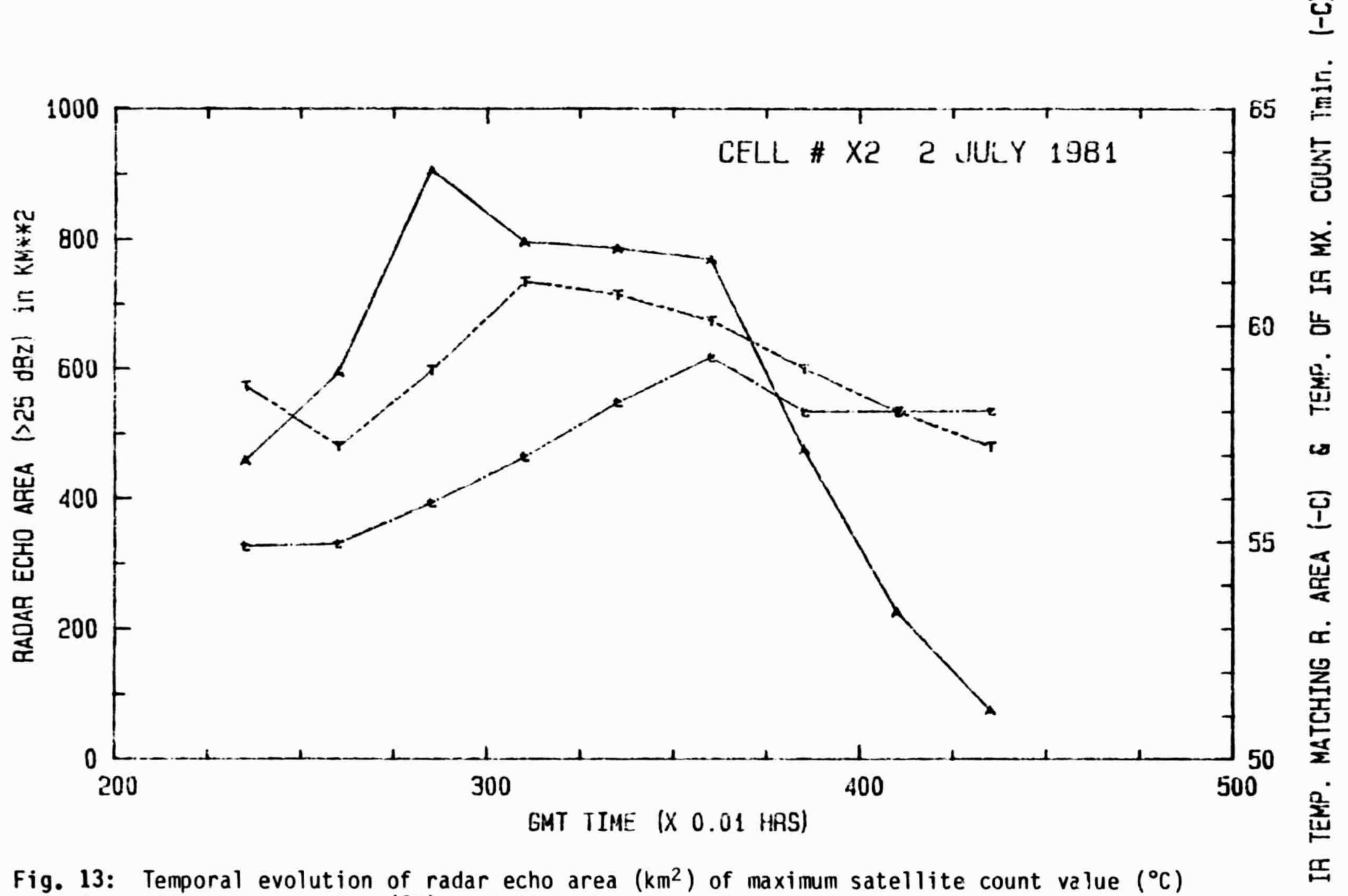

Fig. 13: Temporal evolution of radar echo area (km^2) of maximum satellite count value (°C) and of satellite count value (°C), matching the interpolated radar area multipled with time increment for cluster X2.

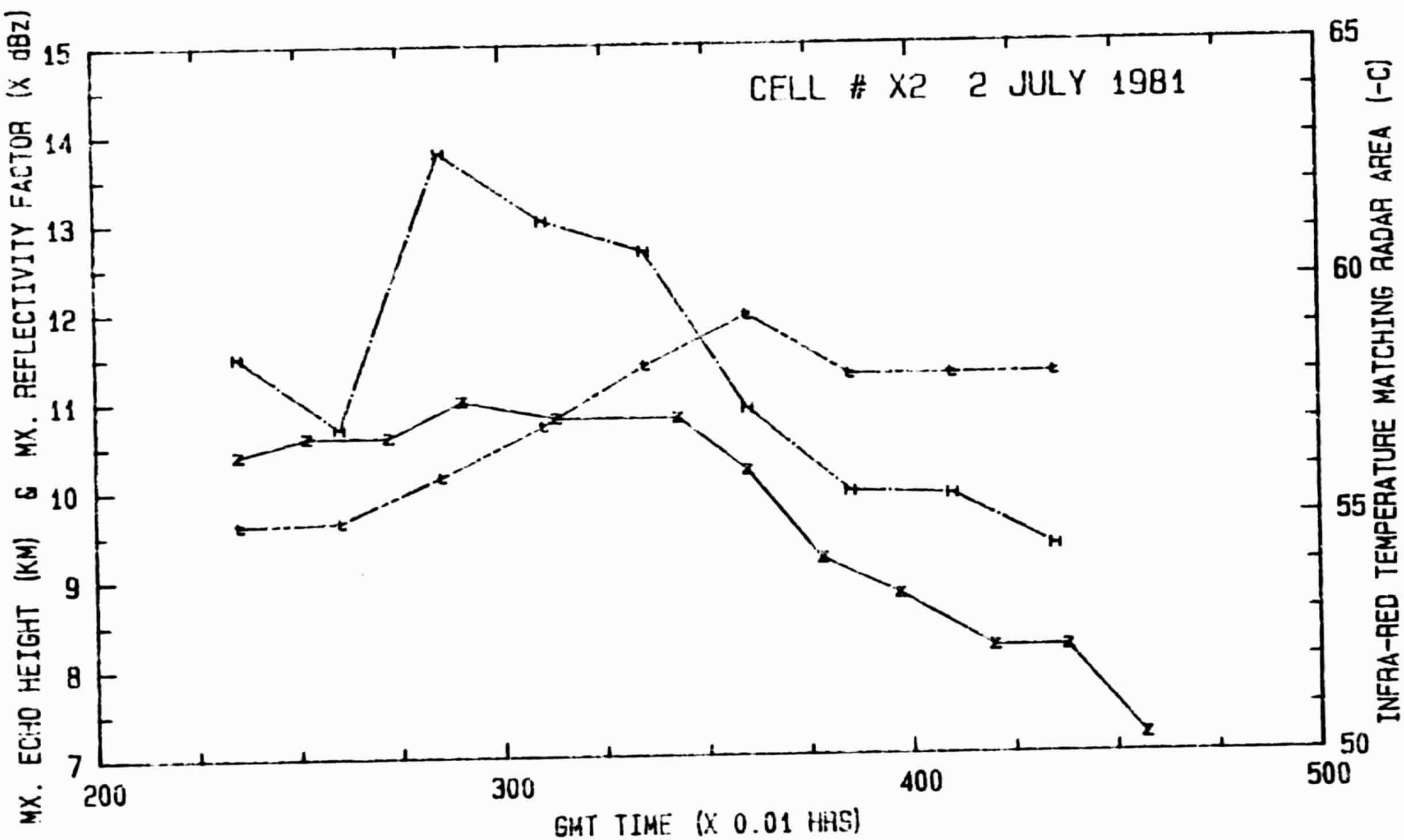

Fig. 14: Temporal evolution of maximum echo height. of maximum reflectivity factor (dBz) and of satellite count value (°C), matching the interpolated radar area multiplied with time increment for cluster X2.

TABLE 6

GOES Satellite and Bowman Radar Data for Four Clusters
(Two on 12 June and Two on 2 July) of Summer 1981

Date	Cell No.	λ	Satellite Count Threshold Matching Radar ATI	Satellite IR Temp. Matching Radar ATI T_{Ma}	Satellite IR Maximum Count Value (°C) T_{Mx}	Satellite Averaged* Maximum Count Value (°C) T_{AMx}	Max. Echo Height (km) MEh
12 Jun	1A	VIS	57.2				
		IR	177.9	-33.1	-50.2	-39.8	12.2
12 Jun	1B	VIS	58.9				
		IR	186.7	-41.9	-49.2	-37.6	12.1
2 Jul	X1	IR	201.4	-56.6	-59.2	-54.0	12.5
2 Jul	X2	IR	202.9	-58.1	-61.2	-58.6	14.4

*Averaged over the cell lifetime.

A paper entitled "An Attempt to Extend the ATI Technique to Estimate Convective Rain Volumes Using Satellite Data" coauthored by A. A. Doneaud, J. R. Miller, Jr., L. R. Johnson (SDSM&T), and T. H. Vonder Haar and P. Laybe (CSU) was presented in a poster session and included in the preprint volume of the 22nd Conference on Radar Meteorology, 10-13 September 1984, Zurich, Switzerland (Attachment 1).

Statements are included in the last papers acknowledging NASA's support of the research grant. A list of consulted bibliographic references is included in the manuscripts published.